SHORT TITLE: GmYSL7, a peptide transporter essential for SNF.

Corresponding author details: Penelope Smith, School of Life Sciences, Agribio, 5 Ring Rd, Bundoora, Victoria, 3083, Australia.

TITLE: Soybean Yellow Stripe-like7 is a symbiosome membrane peptide transporter essential for nitrogen fixation

Gavrin A[2], Loughlin PC[2], Brear EM[2], Griffith OW[6,7], Bedon F[1], Suter Grotemeyer M[4], Escudero V[5], Reguera M[5], Qu Y[2], Mohd-Noor SN[2], Chen C[2], Osorio MB[1], Rentsch D[4], González-Guerrero M[5], Day DA[3], Smith PMC[1*].

[1]School of Life Sciences. La Trobe University, Bundoora, Victoria 3083. Australia.

[2]School of Life and Environmental Science, The University of Sydney, Sydney, New South Wales, 2006, Australia

[3]College of Science and Engineering, Flinders University, Bedford Park, Adelaide, SA, Australia

[4]IPS, Molecular Plant Physiology, University of Bern, Altenbergrain 21, 3013 Bern Switzerland

[5]Centro de Biotecnología y Genómica de Plantas (UPM-INIA). Universidad Politécnica de Madrid. Campus de Montegancedo. Crta. M-40 km 38. 28223 Pozuelo de Alarcón (Madrid), Spain

[6]School of BioSciences, University of Melbourne, Parkville, VIC, Australia

[7]Department of Biological Sciences, Macquarie University, Macquarie Park, NSW, 2109

One sentence summary: GmYSL7 is a symbiosome membrane peptide transporter that is essential for symbiotic nitrogen fixation that when silenced blocks symbiosome development.

Author contributions: AG completed the gene silencing, RNAseq analysis and contributed to the localisation. PCL cloned the gene and contributed to the localisation, promoter GUS analysis and real time analysis. EMB, SNMN, MSG, DR

and PMCS completed the analysis of YSL7 in yeast. OG, EMB, MBO, FB and PMCS analysed the RNAseq results. VE, MR and MGG completed the complementation of MtYSL7. YQ completed the real time analysis. CC completed the promoter GUS analysis. PMCS, FB, EMB and DAD isolated symbiosome and microsomal membrane and did proteomic analysis. PMCS and DAD conceived the project and were involved in experimental design and analysis. PMCS and AG wrote the manuscript. All authors contributed to editing of the manuscript.

Funding information : This research was funded by the Australian Research Council Discovery Projects DP0772452, DP120102780 and DP150102264 and Industrial Transformation Research HUB IH140100013.

ABSTRACT

Legumes form a symbiosis with rhizobia that convert atmospheric nitrogen (N_2) to ammonia which they provide to the plant in return for a carbon and nutrient supply. Nodules, developed as part of the symbiosis, harbor rhizobia which are enclosed in the plant-derived symbiosome membrane (SM), to form a symbiosome. In the mature nodule all exchanges between the symbionts occur across the SM. Here we characterize GmYSL7, a member of Yellow stripe-like family which is localized to the SM in soybean nodules. It is expressed specifically in nodule infected cells with expression peaking soon after nitrogenase becomes active. Although most members of the family transport metal complexed with phytosiderophores, GmYSL7 does not. It transports oligopeptides of between four and 12 amino acids. Silencing of GmYSL7 reduces nitrogenase activity and blocks development when symbiosomes contain a single bacteroid. RNAseq of nodules in which GmYSL7 is silenced suggests that the plant initiates a defense response against the rhizobia. There is some evidence that metal transport in the nodules is dysregulated, with upregulation of genes encoding ferritin and vacuolar iron transporter family and downregulation of a gene encoding nicotianamine synthase. However, it is not clear whether the changes are a result of the reduction of nitrogen fixation and the requirement to store excess iron or an indication of a role of GmYSL7 in regulation of metal transport in the nodules. Further work to identify the physiological substrate for GmYSL7 will allow clarification of this role.

INTRODUCTION

Legumes form a symbiosis with soil bacteria, rhizobia, that allows them to access N_2 from the atmosphere. This symbiosis is an important contributor to the biological nitrogen cycle. The rhizobia fix N_2 via the enzyme nitrogenase to produce ammonia and provide it to the plant in return for reduced carbon generated via photosynthesis. This biological N_2-fixation provides a large proportion of the nitrogen in the natural environment (Fowler et al., 2013) and is an important component of sustainable agricultural systems, reducing the requirement for expensive nitrogen fertilizers and the pollution that can arise from their overuse (Vance, 2001).

The establishment of this symbiosis involves signaling between the two partners and results in rhizobia moving through an infection thread derived from an invaginated root cell wall into the root cortex where a new organ, the nodule is initiated. The cell wall of the root cells is degraded and the rhizobia released into the cell. Within the nodule infected cells, the rhizobia are enclosed in a plant-derived membrane to form an organelle-like compartment called the symbiosome. Within this symbiosome the rhizobia differentiate into their symbiotic form, the bacteroid. The symbiosome membrane (SM), initially derived from the plasma membrane (PM), becomes specialized as an interface between the bacteroid and its plant host, segregating the bacteroids from the plant cytoplasm and "protecting" them from any plant defense response (Mohd-Noor et al., 2015).

The major metabolite exchange across the SM is fixed nitrogen (principally ammonia) to the plant and a carbon source, most likely malate, to the bacteroids. However, transport of many other compounds into the symbiosome across the SM must occur as the enclosed bacteroids depend on the plant for all of their nutrients, including iron, zinc, calcium and cobalt amongst others (Brear et al. 2013; Udvardi and Poole, 2013; Clarke et al., 2014). The SM effectively controls the symbiosis via a suite of transport proteins synthesized by the plant. The plant can control what moves into the symbiosome and, presumably, can withhold sustenance if required. It has been suggested that the plant can impose sanctions on non-fixing rhizobia (Kiers et al., 2003) and controlling transport across the symbiosome membrane could regulate this. It is also probable that compounds other than ammonia/ammonium move from the bacteroids to the plant (Udvardi and Poole 2013).

Transport studies with isolated symbiosomes have demonstrated the presence of a malate transporter and an ammonium channel on the SM, as well as metal ion transporters, but their molecular identity remains elusive (Udvardi and Day, 1997; Udvardi and Poole 2013; González-Guerrero et al. 2016). A number of proteomic analyses of the SM have been reported (Wienkoop and Saalbach, 2003, Catalano et al. 2004, Clarke et al. 2015) and although the earlier studies were limited by the lack of genome sequences for the legumes studied, an array of putative transport proteins have been identified. An example is LjSST1, a sulphate transporter later shown to be essential for nitrogen fixation in the *Lotus japonicus*- rhizobia interaction (Krussell et al. 2005; Schneider et al. 2019).

The most recent analysis of the soybean SM proteome (Clarke et al. 2015) identified a protein from the Yellow Stripe-like (YSL) family, Glyma.11G203400 (known then as Glyma11g31870). YSL proteins are members of the wider oligopeptide transporter family, generally considered to transport metals chelated to phytosiderophores (PS), such as deoxymugineic acid and nicotianamine (NA) (Curie et al., 2009). In monocots, PS excreted to the rhizosphere chelate ferric iron and the complexes are transported into the plant cytoplasm by YSL transporters. Maize mutants for the first characterized member of this family show a phenotype of interveinal chlorosis that is characteristic of iron deficiency and it is this phenotype that gave rise to the name Yellow-stripe 1 (YS1). YSL proteins, often localized in xylem parenchyma, can also transport other metal chelates (Dai et al. 2018; Chu et al., 2010; Sasaki et al., 2011, Zheng et al. 2012) and are important for intracellular iron transport and iron homeostasis, with both ferric and ferrous-PS complexes transported (Lubkowitz, 2011). YSL proteins are also involved in mobilization of intracellular stores of metals (Divol et al. 2013, Conte et al. 2013). YSL transporters operate through proton co-transport driven by the membrane potential (Schaaf et al. 2004) and whether localized to the PM or internal membranes, transport is always into the cell cytosol (Lubkowitz 20ll).

Despite the biochemical characterization of some members of the YSL family, the functional role of other members is less clear. In particular, members of one phylogenetic clade of the YSL family, including YSL5, 7 and 8 (Group III) are not

well characterized. A recent study showed that Arabidopsis YSL7 and 8 are responsible for the import of a *Pseudomonas syringae* virulence factor, syringolin A (Syl A), into the plant cytoplasm where it inhibits the proteasome (Hofstetter et al. 2013). Syl A is a peptide derivative and peptides of 4-8 amino acids in length were able to inhibit its transport in plants and in yeast expressing AtYSL7. Consequently, it was suggested that AtYSL7 and AtYSL8 act as oligopeptide transporters, although direct evidence of oligopeptide transport was not shown (Hofstetter et al. 2013).

In this study we show that both AtYSL7 and GmYSL7 (encoded by Glyma.11G203400) can transport oligopeptides and that the soybean protein, which is localized to the SM in nodule infected cells, is essential for nitrogen fixation.

RESULTS

GmYSL7 is a transporter of the YSL family

In our proteomic study (Clarke et al., 2015) we identified Glyma.11G203400 on the SM of soybean nodules. The protein is a member of the oligopeptide transporter (OPT) superfamily (Saier, 2000; Yen et al., 2001; Stacey et al., 2008) and has significant homology with members of the YSL family (Curie et al. 2009). We named it YSL7, as its closest Arabidopsis homologue is AtYSL7 (74% amino acid identity and 85% similarity; Yorden et al. 2011).

GmYSL7 belongs to a family consisting of 15 members in soybean (Supplementary Fig. S1; Schmutz et al., 2010) which in phylogenetic analysis fall into the three clades with both monocots and dicots members (Groups I – III, Supplementary Fig. S1). Group IV has only monocot members. In Genbank six proteins are annotated as "probable metal-nicotianamine transporter YSL7" but in the phylogenetic analysis only GmYSL7, Glyma.11G203400, associates closely with AtYSL7 in Group III, also clustering with the chickpea protein CaYSL7 (Ca08876) and three *M. truncatula* proteins (Medtr3g063490 [MtYSL7], Medtr3g063520 [MtYSL9] and Medtr5g091600 [MtYSL8]) (Supplementary Fig. S1). Of the other soybean proteins annotated as YSL7, Glyma.09G164500 and Glyma.16G212900 are more closely related to AtYSL5 and AtYSL8, while Glyma.09G281500, Glyma.20G004200 and Glyma.20G004300, although part of Group III, form a sub-clade not associated with any YSL proteins from other plants included in the phylogeny (Supplementary Fig. S1).

GmYSL7 is expressed in infected cells of soybean root nodules

Publicly available transcriptomic data for soybean suggests nodule-specific expression of *GmYSL7* (Severin et al. 2010; Supplementary Fig. S2). We confirmed this by measuring *GmYSL7* transcript abundance in leaves, roots of 8-day old seedlings, nodules and denodulated roots of 32-day-old plants using quantitative reverse transcription (RT-q) PCR. *GmYSL7* transcript was abundant in nodules but almost undetectable in other plant organs examined (Fig 1A). We investigated the expression patterns of other YSL genes and all had lower nodule expression than *YSL7* and transcripts present in other tissues (Supplementary Fig. 2).

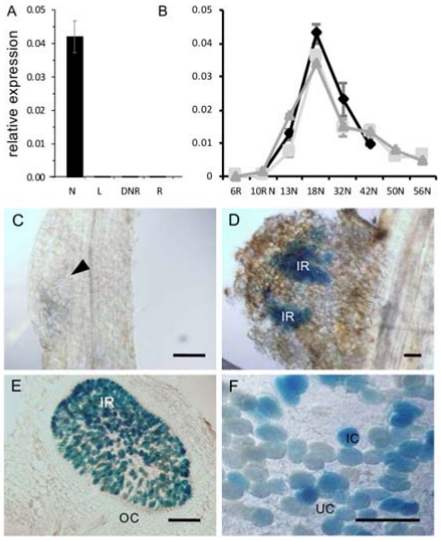

Figure. 1 GmYSL7 is expressed in infected cells of soybean root nodules. A. Transcript level of GmYSL7 in tissue samples from different organs. N, nodules; L, leaves; DNR, denodulated roots; R, roots. B. Transcript level of GmYSL7 during nodule development. 6R, roots 6 days after inoculation (DAI); 10RN, roots and nodules 10 DAI; 13N-26N, nodules the indicated DAI. Data shown are for three independent time courses. Bars, SE (n = 3). Nitrogenase activity was first detected at 18 DAI. C. Transgenic root expressing pYSL7:GFP-GUS. GUS staining was not detectable in the very early stages of nodule development. Arrowhead indicates a nodule initiation. D. Transgenic pYSL7:GFP-GUS 10-day-old nodule primordia. IR, infected region. E. Transgenic pYSL7:GFP-GUS mature nodule. GUS staining is restricted to infected cells. OC, outer cortex. F. Magnification of E. Scale bars, 150 µm.

Expression of *GmYSL7* during nodule development was examined with mRNA essentially undetectable in young (6 – 10-day-old) inoculated roots; however, transcript abundance increased sharply before nitrogenase activity was first detected (day 18; Supplementary Fig. 3), peaking in nodules from 18-day-old plants, and steadily decreased after this time (Fig. 1B).

As some characterized YSL proteins are involved in transport of iron complexes we examined expression of *GmYSL7* in nodules grown under varied (0 – 100 µM) added iron conditions. Two replicates were completed and although the level of expression was slightly lower in the second (not shown), the pattern of expression was similar. *GmYSL7* expression was largely insensitive to iron concentration (Supplementary Fig. 3). This was in contrast to an *AtYSL3* homologue with clear upregulation in high iron conditions (results not shown).

We investigated *GmYSL7* cellular expression pattern and the subcellular localization of the expressed protein in nitrogen-fixing nodules. The 2 kb genomic fragment immediately upstream of the coding region of GmYSL7 was inserted upstream of a promoter-less green fluorescent protein-*β*-glucuronidase (GFP-GUS) coding region to give *pGmYSL7:GFP-GUS*. GUS staining of *pGmYSL7:GFP-GUS* transformed roots

and nodules agreed well with our RT-qPCR data, with no staining detectable in roots or in early nodule initials (Fig. 1C). GUS staining became evident as nodules developed (Fig. 1D) and was strongest in maturing nodules. In mature nodules, GUS staining was detected in the infected region and appeared to be confined to rhizobia-infected cells (Fig. 1E and F). No GUS staining was detected in the outer cortex of the nodule (Fig. 1E) or in untransformed nodules (data not shown).

Localization of GmYSL7 on the SM in rhizobia-infected cells was confirmed using transgenic nodules expressing *pGmLBc3:GFP-GmYSL7* and analysed by confocal microscopy. FM4-64, a lipophilic dye that fluoresces when bound to membrane (Vida and Emr, 1995), was used to counterstain the SM (Limpens et al. 2009, Gavrin et al. 2014). GFP-GmYSL7 signal was on internal membranes within infected cells but not on the PM (Fig. 2B, D). Co-localization of GFP and FM4-64 (Fig. 2A-C) signals indicates discrete localization of GFP-GmYSL7 on the SM as can be seen also in Fig 2D, with GFP-YSL forming a clear "halo" around the perimeter of symbiosomes. The GFP-YSL7 fluorescence pattern in infected cells (Fig 2D) was distinct from free GFP, detected in the cytoplasm (Fig. 2E), and from that of a construct targeted to the symbiosome space (Fig. 2F).

Further confirmation that GmYSL7 was localized on the SM and not the PM was obtained by proteomic analysis of isolated SM and microsomal extract enriched in PM and endoplasmic reticulum. Approximately six times more peptides from the well characterized, SM-localized GmNOD26 were in the SM sample compared to the microsomal membrane sample, indicating enrichment of the SM in the purified sample. GmYSL7 peptides were only in the purified SM sample (Supplementary Table 1).

Silencing of GmYSL7 interrupts development of the symbiosis

Since GmYSL7 is localized to the SM, we investigated whether it is essential for development of the symbiosis and nitrogen fixation by rhizobia using RNA interference (RNAi). Nodules from transgenic roots silenced for GmYSL7 were analyzed 24 days post inoculation (dpi; Fig. 3C). Expression of *GmYSL7* in RNAi nodules was approximately 40% of the control but expression of the closest homologs, *Glyma.16G212900 (GmYSL8)* and *Glyma.09G164500 (GmYSL5)*, was not

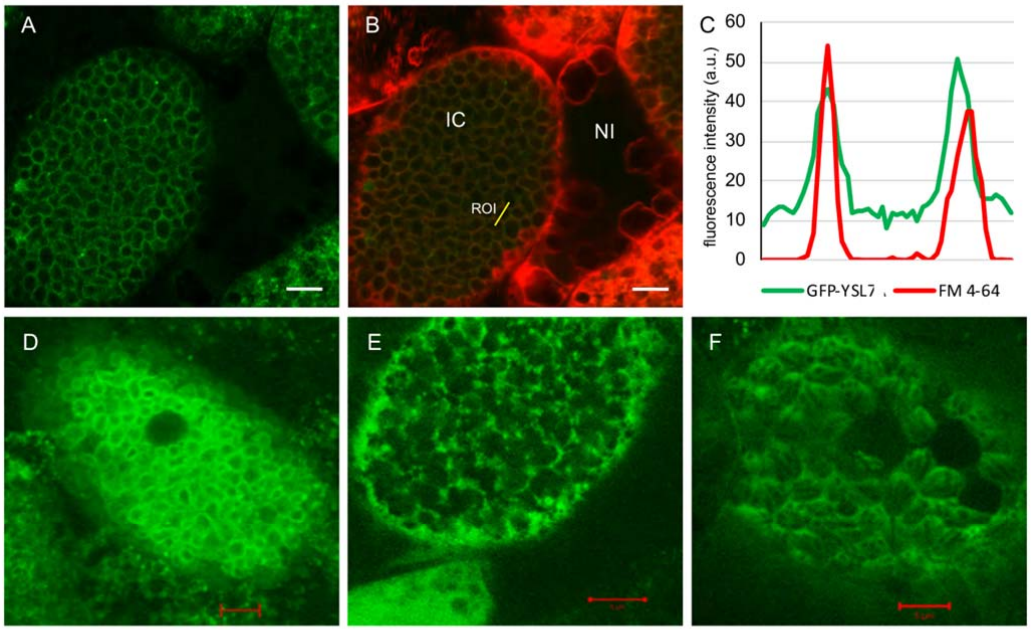

Figure 2. Localization of GmYSL7 in soybean nodule cells infected with rhizobia. A. GFP-GmYSL7 localizes on symbiososme membranes in infected cell of soybean nodules. B. Colocalization of GFP-YSL7 with membrane lipophilic dye FM4-64 in the same cell. IC, infected cell; NI, non infected cell; ROI, region of interest. C. Fluorescent intensity plot of ROI from B. D. Superimposed confocal image of GFP-GmYSL7 signal on the symbiosome membrane in rhizobia-infected nodule cells. E. Free GFP localizes to the cytoplasmic spaces surrounding symbiosomes in infected cells. F. MtNOD25-GFP (Hohnjec et al. 2009) localizes to the peribacteroid space inside the symbisomes. Scale bars, 5µm.

affected (Fig. 3C). Acetylene-reduction analyses showed that nitrogenase activity was reduced in silenced nodules to only 25% of the activity of control nodules (Figure 3D). *GmYSL7* silenced nodules were smaller (Fig. 3E) and displayed a delay in development (Fig. 3A, B) in comparison to empty vector control nodules (Fig. 3 G-H).

Silencing of *GmYSL7* did not affect bacteria release, but infected cells remained small and, unlike the control nodules, contained small, single-bacteroid symbiosomes (Fig. 3B). Numerous small vacuoles were localized around the nucleus (Fig. 3F) whereas control nodules had no vacuoles (Fig. 3H). To pinpoint the developmental stage in wild type nodules that matches the RNAi nodules we completed an analysis of nodules from soybean infected with *Bradyrhizobium diazoefficiens* strain 1042-45

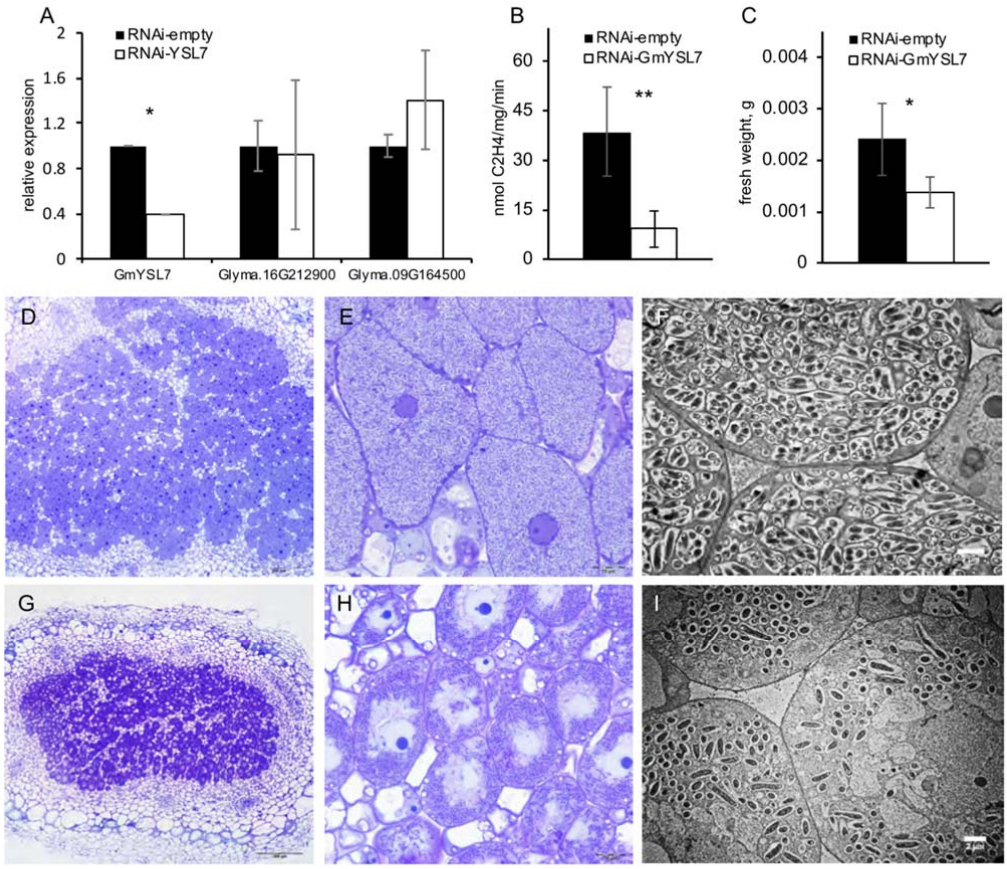

Figure 3. RNAi silencing of GmYSL7 affects nodule development. A. Transcript level of GmYSL7 and its closest homologs in 24-day-old nodules of empty vector control and RNAi-GmYSL7 plants (error bars represent SD; n=4; t-test: *, $p<0.05$). B. Nitrogenase enzyme activity in 24-day-old nodules of empty vector control and RNAi-GmYSL7 plants (error bars represent SD; n=8; t-test: **, $p<0.01$). C. Fresh weight of 24-day-old nodules of empty vector control and RNAi-GmYSL7 (error bars represent SD; t-test: *, $p<0.05$). D. Longitudinal section of a 24-day-old nodule from an empty vector control plant. E. Magnification of (A) showing developed (stage IV) infected cells. F. Electron microscopy of infected cells of a 24-day-old nodule from empty vector control containing developed multibacteroid symbiosomes. G. Longitudinal section of a RNAi-GmYSL7 24-day-old nodule. H. Magnification of (D) showing undeveloped (stage II) infected cells. I. Electron microscopy of infected cells of a RNAi-GmYSL7 24-day-old nodule containing undeveloped single-bacteroid symbiosomes. Scale bars as indicated.

carrying the *lacZ* fusion driven by the *nifD* promoter (Acuña et al., 1987). Four stages of development were identified and images can be seen in Supplementary Fig. 4. The morphology of infected cells of *GmYSL7*-silenced nodules (Fig. 3B) appeared to be arrested at stage II of normal nodule development (Fig. 3F, Supplementary Fig. 4B, F) where numerous small vacuoles were present in infected cells and most symbiosomes contained single elongated bacteroids. Electron microscopy (EM) of the silenced nodules confirmed that the infected cells were small and under-developed, packed with symbiosomes containing only a single bacteroid (Fig. 3). Bacteroids appeared

elongated as seen in control nodules during stage II (Supplementary Fig. 4F). Infected cells also contained numerous vacuoles of different sizes and apparent endosomes fusing with symbiosomes, reminiscent of the formation of a lytic compartment, which usually occurs during nodule senescence (Fig. 3I). Symbiosomes were isolated from silenced and control nodules, and this showed that in the silenced nodules, symbiosomes contained only single bacteroids compared to the control symbiosomes, which had multiple bacteroids (Supplementary Fig. 4), confirming the phenotype seen by EM analysis. The results suggest that silencing of *GmYSL7* arrests development of soybean nodules at stage II.

RNAseq of nodules in which *GmYSL7* is silenced

We used RNAseq to compare the transcriptome in 22-day old nodules from *GmYSL7*-RNAi plants and empty vector controls. In these experiments, *GmYSL7* expression in RNAi plants was around half that of control expression. Principal component analysis (Fig. 4A) and a heatmap of gene expression of all differentially expressed genes shows clear differences between the RNAi and control samples (Fig. 4B). There were no significant changes in expression of other YSL genes.

There were 924 genes with $\log_2$fold change of 1 or greater in nodules in which YSL7 was silenced, while 1180 genes had $\log_2$fold change of -1 or greater (with adjusted p-valiue <0.05). Gene ontology (GO) enrichment analysis showed that genes involved in defence responses (e.g. defence response to bacterium, defence response to other organism), "negative regulation of endopeptidase activity" and a network associated with iron homeostasis, sequestration and transport, are overrepresented in the upregulated genes (Fig. 4C). A network of genes with GO terms associated with regulation of transcription and signal transduction, and another including those associated with lipid biosynthesis, are overrepresented in the downregulated transcripts (Fig. 4D).

Details of expression of particular genes in the RNAi and control nodules are available in Supplementary Table 2. Among the genes with significantly higher expression in the silenced nodules were those encoding homologues of a senescence-associated gene 13 (Glyma.12G059200), NRT1.8/NPF7.2 (proton-coupled H+/K+ antiporter, Glyma.18G260000), organic cation/carnitine transporter4

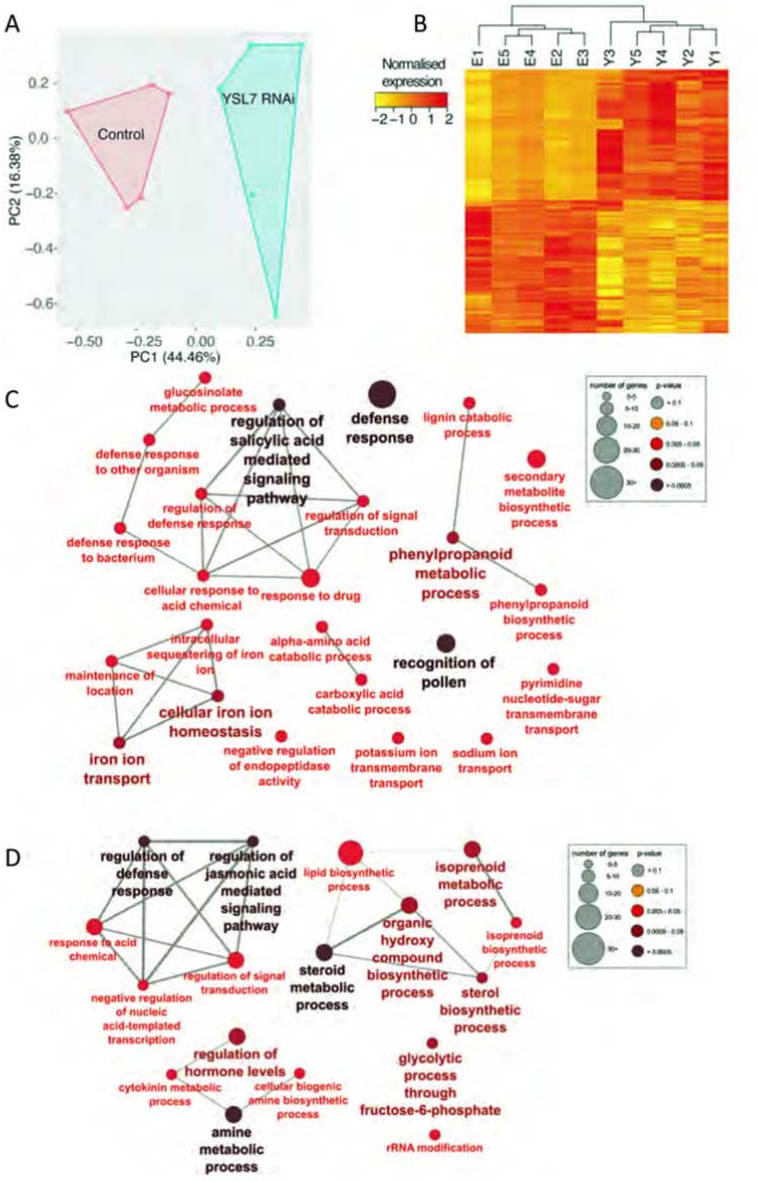

Figure 4. RNAseq analysis of *GmYSL7*-RNAi nodules. A. Principal component analysis of RNAseq samples. B. Heatmap of clustering of differentially regulated genes in each nodule sample. C, D. Gene Ontology enrichment analysis of biological processes in up (C) and down (D) regulated genes from GmYSL7 RNAi nodules. GO term enrichment analyses were performed using the ClueGO v2.5.5 plugin (Bindea et al., 2009) in Cytoscape v3.5.1 (Shannon et al., 2003). Circles represent an enriched group of genes based on their GO terms. Circle size and colour indicate the number of mapped genes and associated Term PValue corrected with Bonferroni step down.

(Glyma.12G216400), ferritin (Glyma.01G124500, Glyma.11G232600, Glyma.03G050100), vacuolar iron transporter-like proteins (Glyma.05G121200, Glyma.08G076000), plantacyanin (Glyma.08G128100), a copper transport protein (Glyma.09G179800), cation efflux family protein (Glyma.08G164800), a cationic

amino acid transporter 2 (Glyma.19G116500), nitrate transporter 2.4 (Glyma.11G195200) and a number of protease inhibitors (Supplementary Table 2).

Genes with significantly lower expression in the *GmYSL7* silenced nodules were those encoding homologues of sucrose-proton symporter 2 (Glyma.16G156900), glutamine dumper 2 (Glyma.18G277600), nicotianamine synthase 1 (NAS, Glyma.15G251300), GmNIC1a (Glyma.12G208900), a Clavata3/ESR (CLE) related homologue, and Putative lysine decarboxylase family protein (Supplementary Table 2).

GmYSL7 transports oligopeptides and Syringolin A but not Fe(II)-NA

Yeast complementation was used to try to identify a substrate for GmYSL7. Initially we tested for transport of Fe(II)-NA by complementation of the *fet3/fet4/ftr1* mutant; however, although the positive control *ZmYS1* (Curie et al. 2001, Schaaf et al. 2004) complemented the mutant, *GmYSL7* and *AtYSL7* did not (Fig. 5).

Since the YSL family is part of the wider oligopeptide transporter (OPT) family, we next tested whether GmYSL7 could complement the yeast oligopeptide transport *opt1* mutant, using different oligopeptides as the sole source of nitrogen for growth. When the transformants were grown with four (ALAL, LSKL), five (IIGLM) and six (KLLLLG) amino acid peptides as the only N source, cells expressing AtYSL7, GmYSL7 or AtOPT4, but not with the empty vector pDR196, grew (Fig. 6). On media containing larger peptides (eight, ten or twelve amino acid), the growth of the transformants was more varied. AtOPT4 supported growth on the eight amino acid peptide DRVYIHPF, while growth was weak for AtYSL7 and GmYSL7. Growth on the 10 amino acid peptides DRVYIHPFHL was close to background for all transformants, but all grew better than vector control on the 12 amino acid peptide RLAPEGPDPHHN (Fig 6) which corresponds to the mature CLE peptide, GmRIC1a (encoded by Glyma.13G292300; Hastwell et al. 2015).

AtYSL7 is involved in syringolin A (SylA) uptake and, when expressed in yeast, exposure to SylA inhibited growth (Hofstetter et al. 2013, Fig. 7) suggesting the transporter mediated uptake of this toxic peptide derivative. We used this assay to test for transport of SylA by GmYSL7. GmYSL7, AtYSL7 and the empty vector pDR195

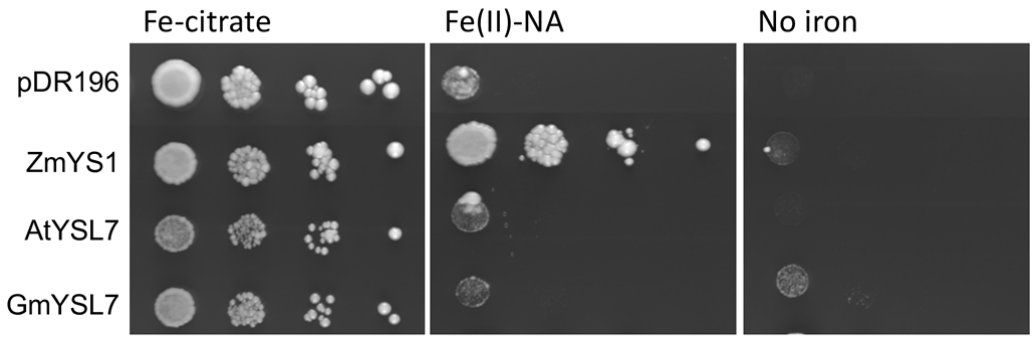

Figure 5. GmYSL7 does not transport Fe(II)-nicotianamine (NA). DEY1530 yeast (*fet3/fet4/ftr1*) was transformed with the empty vector plasmid pDR196, *AtYSL7, GmYSL7, ZmYS1* in pDR196-GW. Serial dilutions of each yeast transformant were applied to SD plates (that include 1.6 μM $FeCl_3$) with 10 μM Fe-citrate, Fe(II)-NA or no added iron (no iron) and the plates grown for 3-5 days.

were expressed in the yeast *pdr5* mutant, that lacks the ABC transporter PDR5, and plated as a lawn (Hofstetter et al., 2013). When a disk containing SylA was placed on the plate, growth of yeast expressing GmYSL7 and AtYSL7, but not the empty vector pDR195, was inhibited. Inhibition of growth caused by SylA on the AtYSL7 plate showed as clear patches on the plate for all concentrations of SylA tested, while inhibition of yeast expressing GmYSL7 was weaker (Fig. 7).

GmYSL7 and MtYSL7 are functionally equivalent

In the accompanying manuscript (Castro-Rodríguez et al. 2020), MtYSL7, which is localized on the PM in the vasculature and nodule cortex in *Medicago truncatula*, is described. To determine whether GmYSL7 and MtYSL7 proteins play similar roles in the different cell types in which they are located, we expressed *GmYSL7* in the *Mtysl7* mutant. Expression was driven by the *MtYSL7* promoter to ensure expression in the cells in which MtYSL7 is present (vasculature and nodule cortex but not infected cells). Although GmYSL7 localizes to the SM in soybean, it was able to complement the *Mtysl7* transposon insertion mutant to restore nitrogenase activity to wild type levels and increase the dry weight of the transformed plants compared to the mutant (Fig. 8). Based on this result, we assume that in the *Mtysl7* mutant, when expressed in the cells where MtYSL7 is normally active, GmYSL7 at least partially localizes to the PM.

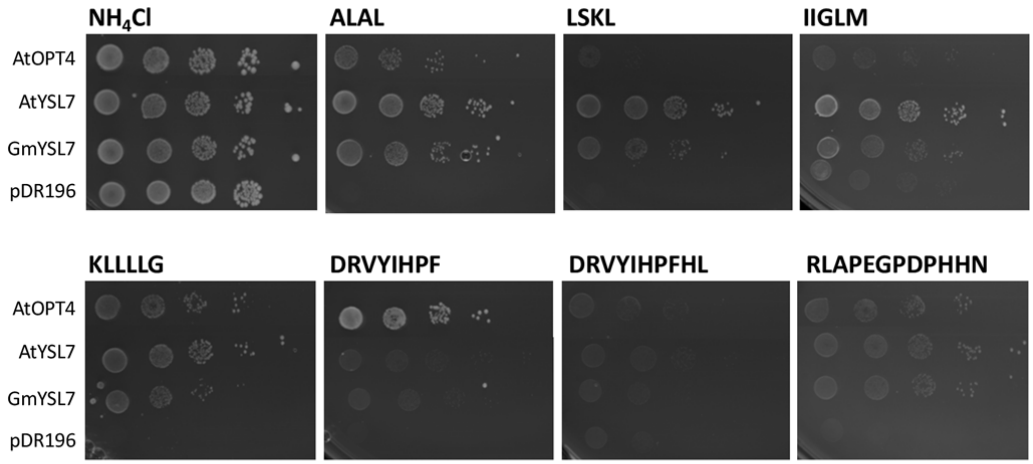

Figure 6. GmYSL7 and AtYSL7 transport oligopeptides. *AtOPT4, AtYSL7, GmYSL7* in pDR196-GW and the empty vector (pDR196) were introduced into the yeast *opt1* mutant, Y11213. Serial dilutions of each transformant were grown as above on minimal medium containing either 10 mM NH_4Cl (positive control) or 100 µM peptide (with sequence as indicated) as the sole source of nitrogen

348

349

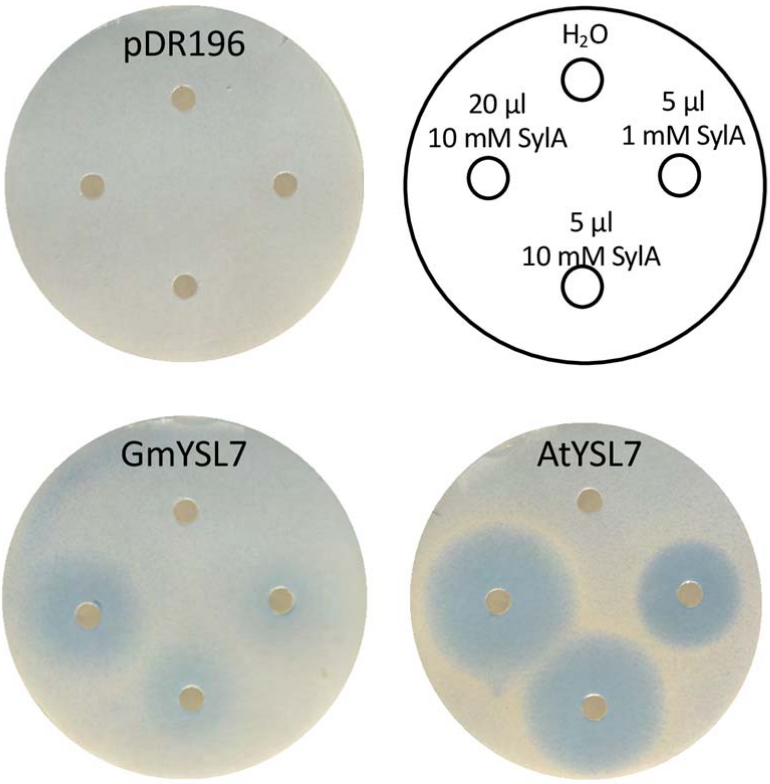

Figure 7. GmYSL7 transports Syringolin A. BY4742 yeast *Δpdr5:KanMX6* transformed with the empty vector (pDR196) or the vector expressing *AtYSL7* or *GmYSL7* were plated as a lawn on solid synthetic defined (SD) media. Filter disks with the indicated SylA solutions were placed onto the plates and inhibition of growth examined after 2 days.

DISCUSSION

We have characterized a member of the YSL family, GmYSL7, in soybean. The protein is part of a clade of YSL proteins (Group III) that includes AtYSL5, AtYSL7 and AtYSL8. AtYSL7 and 8 are involved in transport of the *Pseudomonas syringae* virulence factor into Arabidopsis cells across the PM (Hofstetter et al. 2013), but their physiological role in plants has not been determined. GmYSL7, AtYSL7, CaYSL7 and three *Medicago truncatula* proteins (MtYSL7, 8 and 9) form a cluster in phylogenetic analyses, but the soybean protein's expression profile is distinct from that of *AtYSL7* and *MtYSL7*. *AtYSL7* is expressed mainly in flowers but also in siliques and roots. *MtYSL7*, has highest expression in nodules, but is also expressed in roots. Soybean, on the other hand, appears to lack a *YSL7* paralog with expression

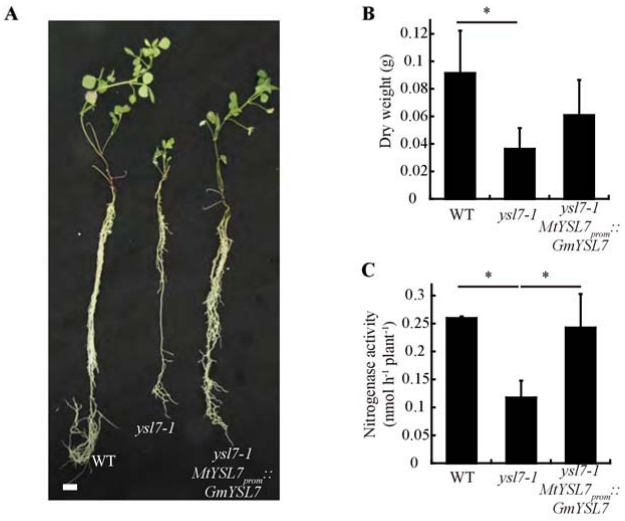

Fig. 8. GmYSL7 is functionally equivalent to MtYSL7. A) Growth of representative wild type (WT), *ysl7-1*, and *ysl7-1* transformed with *GmYSL7* controlled by the *MtYSL7* promoter (*ysl7-1 MtYSL7*$_{prom}$*:: GmYSL7*). Bar = 1 cm. (B) Dry weight of 28 dpi WT, *ysl7-1*, and *ysl7-1 MtYSL7*$_{prom}$*:: GmYSL7* plants. Data are the mean ± SE of 5 transformed plants. (C) Nitrogenase activity of 28 dpi WT, *ysl7-1*, and *ysl7-1 MtYSL7*$_{prom}$*:: GmYSL7* plants. Acetylene reduction was measured in duplicate from two sets of three-four pooled plants. Data are the mean ± SE. * indicates statistically significant differences ($p<0.05$)

similar to *AtYSL7* and *MtYSL7*. Rather, *GmYSL7* expression is linked specifically to symbiotic nitrogen fixation, occurring only in infected nodule cells where the protein is present on the SM, but not the PM, in contrast to AtYSL7 and MtYSL7. Furthermore, its expression is only marginally affected by the iron concentration of the growth medium (Fig S4). This seems a clear example of neofunctionalization with the loss of the paralog (Xu et al. 2017). Either there is no requirement in soybean for the role played by AtYSL7 in other organs or another soybean gene with functional redundancy fulfils that role. The closest homologues of *GmYSL7*, *Glyma.16G054200* (*GmYSL8*) and *Glyma.19G094800* (*GmYSL5*) are expressed in almost all tissues (Fig. S2), but we know nothing about their function at this stage.

An important role for GmYSL7 in nitrogen-fixing nodules is shown by knockdown of its expression, which resulted in smaller nodules and a decrease in nitrogenase activity. The *GmYSL7* RNAi nodules appear to have been developmentally arrested, with small symbiosomes that contain only one bacteroid, in contrast to the large

symbiosomes containing multiple bacteroids in infected cells of control nodules. The *GmYSL7* RNAi infected cell ultrastructure is similar to control nodules in the early stages of development. This suggests that the activity of GmYSL7 – and the substrate(s) it transports across the SM - is important for the continued development of the symbiosis and maturation of infected cells.

Our results show clearly that GmYSL7 transports a range of small peptides. When considering the activity of SM transporters, it is important to bear in mind the orientation and energization of the SM (Udvardi and Day, 1997), as this influences the direction that any given substrate is transported. A P-type ATPase on the SM together with the rhizobial electron transport chain, pump protons into the symbiosome space, creating an electrochemical gradient across the SM, with the membrane potential positive on the inside and the interior of the symbiosome (symbiosome space) acidic (Udvardi and Day, 1997). All YSL proteins characterised to date transport compounds across cell membranes into the cytoplasm (Lubkowitz 2011), with proton symport the most likely mechanism (Schaaf et al. 2004). Assuming that GmYSL7 has a similar mechanism, it is consequently likely to transport its peptide substrate out of the symbiosome and into the plant cell cytosol. The phenotype seen in *GmYSL7*-RNAi nodules is, therefore, related to the lack of provision of this substrate to the plant cell.

The *Medicago truncatula* homologue of GmYSL7, MtYSL7, is characterized in an accompanying manuscript and although it is not localized on the SM, the *Mtysl7*-mutant has a phenotype that also affects the symbiosis and nitrogen fixation (Castro-Rodríguez et al. 2020). The difference in cellular localization might be explained by the fact that *M. truncatula* produces indeterminant nodules, where the meristem continues to be active throughout development, and soybean determinant nodules, in which mature nodules have no meristem. As well as structural differences the different nodule types have a number of metabolic differences including in the mechanism for nitrogen assimilation and the compounds transported from the nodules (Smith and Atkins, 2002). However, *GmYSL7* is functionally equivalent to *MtYSL7* because it complemented the *Mtysl7-1* mutant, restoring nitrogenase activity and growth in low N conditions. This suggests that the two YSL7 proteins are able to transport the same substrate/s and that while MtYSL7 brings this substrate into the

cell across the PM, GmYSL7 moves its substrate out of the symbiosome and into the cytosol.

The fact that *GmYSL7* complements the *Mtysl7* mutant also suggests that the mechanism for targeting the GmYSL7 protein to the PM in non-infected cells (where it is expressed from the *MtYSL7* promoter) must be modified in infected cells to allow it to reach the SM. This could involve a chaperone specific to the infected cell but might also be related to the fact that the SM is initially derived from the PM (Brear et al. 2013, Mohd-Noor et al. 2015).

In contrast to many other YSL proteins, neither of the legume YSL7 proteins, nor that from Arabidopsis, were able to transport Fe(II)-NA (this study, Castro-Rodríguez et al. 2020 accompanying manuscript). Additionally MtYSL7 could not transport Fe(III), zinc or copper complexed with NA (Castro-Rodríguez et al. 2020, accompanying manuscript). On the other hand, complementation of the yeast *opt1* mutant showed that the three proteins could transport oligopeptides of various sizes, including a CLE peptide, GmRIC1a. Like AtYSL7, when expressed in yeast, GmYSL7 could also transport syringolin A, a peptide derivative that is the virulence factor for *Pseudomonas syringae* (Hofstetter et al. 2013). Inhibition of yeast growth caused by the transported SylA was not as strong as for AtYSL7 suggesting that GmYSL7 may not transport it as effectively or have the same specificity for the compound. In our assays for direct uptake of oligopeptides in yeast, both AtYSL7 and GmYSL7 supported growth on media with oligopeptides of 4-6 and 12 amino acids as their sole N source, but there was little growth when the 8 amino acid peptide, DRVYIHPF was used, despite its ability to reduce the effect of SylA on Arabidopsis roots (Hofstetter et al., 2013). MtYSL7 was also identified as an oligopeptide transporter and showed similar specificity for oligopeptides to AtYSL7 and GmYSL7 (Castro-Rodríguez et al., 2020 accompanying manuscript).

While it is clear that YSL7 proteins are peptide transporters, their physiological role in legumes is not clear. Glutathione is a three amino acid peptide derivative found in nodules and bacteroids but as MtYSL7 cannot transport GSH (Castro-Rodríguez et al., 2020 accompanying manuscript) and GmYSL7 is able to replace the function of MtYSL7, it is unlikely that transport of GSH out of the symbiosome is the

444 physiological role of GmYSL7. The symbiosome contains a number of proteases on
445 the SM and in the symbiosome space (peribacteroid space; Clarke et al. 2015) and
446 appears to act like a vacuole containing large amounts of free peptides (Clarke et al.
447 2015). Some of these could be substrates for GmYSL7, but why blocking their exit
448 from the symbiosome would inhibit N-fixation and symbiosome development to such
449 an extent is not obvious. While it is possible that GmYSL7 acts to scavenge N by
450 transporting peptides from the symbiosome space into the plant cytosol, it is unlikely
451 that this would have such a profound effect on nodule development.
452
453 It is tempting to speculate that release of peptides from the symbiosomes has a more
454 direct role in manipulating plant gene expression and organogenesis. Cyclic peptides
455 act as signaling molecules in some symbioses (Abbamondi et al. 2014) and it is
456 possible that GmYSL7 transports an oligopeptide derivative produced in the
457 bacteroids. In this scenario, release of the oligopeptide signal could be required to
458 relieve plant inhibition of bacteroid division or as a positive signal for symbiosome
459 development. Supporting this idea is the fact that a protein annotated as an
460 oligopeptide transporter was specifically induced in symbiotic *Bradyrhizobium*
461 *japonicum* (Pessi et al. 2007) and a number of transcription factors are upregulated in
462 nodules of *GmYSL7* RNAi plants.
463
464 We used RNAseq of GmYSL7-RNAi nodules to investigate further the effects of
465 inhibiting transport by GmYSL7. Overrepresented GO terms in the downregulated
466 genes include a range of terms associated with lipid metabolic processes (lipid
467 biosynthetic process, isoprenoid metabolic process). It is likely that this relates to the
468 failure of the symbiosome to develop with multiple bacteroids. The change from a
469 single bacteroid symbiosome to one with multiple bacteroids is likely to require
470 synthesis of large amounts of lipid. With development of the infected cell blocked at
471 an early stage this synthesis would not be required.
472
473 Overrepresented terms in the upregulated genes included “defense response”,
474 “defense response to bacteria”, “defense response to other organism” and “regulation
475 of defense response”, suggesting that blocking transport by GmYSL7 causes a general
476 defense response against the rhizobia. This may be an indirect effect of a decrease in
477 nitrogen fixation, with the plant sanctioning the bacteria for not doing its job (Kiers et

al. 2003). Upregulation of Glyma.11G195200, a soybean homologue of AtNRT2.4, a nitrate transporter that is upregulated in response to nitrogen starvation, suggests that as nitrogenase activity was reduced, the nodules in *YSL7*-RNAi plants were indeed nitrogen starved.

In relation to oligopeptide transport, the gene encoding the CLE peptide GmNIC1a is downregulated (9.3-fold lower) in the RNAi nodules. This peptide is responsible for regulation of nodulation in response to nitrate and its expression is induced by nitrate. Over-expression of the peptide reduces nodulation (Reid et al. 2011), so lower transcript levels might be expected to favour nodule formation and development. It is interesting that YSL7 can transport GmRIC1a, a homologue of GmNIC1a. It is possible that GmRIC1a or a structurally similar peptide is synthesised in the symbiosome and exported via YSL7 to the plant cytosol where it influences nodule development. This would explain the arrested development of nodules in which YSL7 is silenced. If a GmRIC1a-like peptide is a substrate for GmYSL7, then blocking its transport may also affect expression of GmNIC1a gene. In addition to this, the GO term "negative regulation of endopeptidase activity" is overrepresented with higher expression of four protease inhibitors in the RNAi nodules. This may suggest that the peptide transported by YSL7 is processed in the plant cell and blocking its transport leads to expression of inhibitors of proteases.

Another group of GO terms that are overrepresented in the upregulated genes in GmYSL7-RNAi nodules are "intracellular sequestering of iron ion", "iron ion transport" and "cellular iron ion homeostasis". Some of the genes associated with these terms include ferritins and vacuolar iron transporter (VIT) gene homologues. This is accompanied by upregulation of a number proteins potentially associated with metal transport (Cu transport protein, cation efflux family protein, MATE efflux family protein) and a transcription factor, WRKY9, associated with a GO term "cellular response to iron ion starvation". This suggests that metal homeostasis is dysregulated in the *YSL7*-RNAi nodules in a similar manner to that seen in *Mtysl7-2*, where iron and copper concentrations are increased in nodules (Castro-Rodríguez et al. 2020). There are two possible explanations for this. If symbiosome development is stalled and nitrogen fixation blocked, then metals being supplied to the symbiosome by the plant may accumulate in the nodules and need to be sequestered to avoid

cellular damage. This may result in storage, particularly of iron, in uninfected cells with ferritin, or transport into the vacuole via VIT proteins.

Another intriguing effect of the silencing of YSL7 is the downregulation (16-fold decrease) of Glyma.15G251300, a gene encoding NAS, responsible for synthesis of NA, a PS involved in metal transport by YSLs. This is further evidence that YSL7 silencing affects iron homeostasis in the plant (see above). It is also possible that the downregulation in YSL7-RNAi nodules is due to changes in activity of another YSL transporter involved in metal supply to the nodule, but there do not appear to be significant changes in expression of other YSL genes in the RNAi nodules. However, it is also possible that the changes in expression of these genes are simply a consequence of the block in nodule development that occurs in nodules where YSL7 is silenced. Further work is required to definitively answer this.

Another explanation is that GmYSL7 plays a more direct role in metal ion homeostasis, in line with the role proposed by Castro-Rodríguez et al. (2020, accompanying manuscript). If GmYSL7 transports a peptide that signals cellular metal concentrations, then when transport of the peptide ceases the plant may not be able to sense the metal status of the symbiosome, resulting in an iron starvation response in which transcription factors, among them WRKY9, are expressed and upregulate metal transporters, increasing iron transport to the nodules. If simultaneously symbiosome development stalls, these metals may accumulate outside the symbiosome, requiring storage in other forms, such as ferritin. Further study is required to validate these proposals, including the identification of the peptide substrate for GmYSL7.

Conclusion

We have identified a member of the oligopeptide transporter family, GmYSL7, which is localized to the symbiosome membrane in nitrogen-fixing soybean nodules. It transports an array of small oligopeptides out of the symbiosome and into the plant cell cytosol, and its disruption arrests infected cell development and symbiosome maturation, inhibiting nitrogen fixation. It affects expression of a number of genes involved in plant defense responses and in iron homeostasis. It is also able to rescue a

545 *M. truncatula* mutant, in which the equivalent gene is compromised, indicating
546 conserved function across the two legumes.
547
548

METHODS

Plant Growth Conditions

Glycine max L. cv Stevens (soybean) seeds were inoculated at planting and one week after planting with *Bradyrhizobium diazoefficiens* (Soybean group H, New Edge Microbials). Plants were grown as described in Clarke et al. (2015) and fertilized once a week with a nitrogen-free B&D nutrient solution (Broughton and Dilworth 1971). Nitrogenase activity in nodules was assessed using an acetylene reduction assay as described by Unkovich et al. (2008).

For limited and excess iron conditions plants were grown in B&D solution with 0, 1, 10 (control concentration) or 100 µM Fe-citrate, which was renewed every 2 days to maintain pH and stable nutrient supply. Two biological replicates were done. Fe status was determined by elemental analysis (Lee M, School of Land and Environment, University of Melbourne) using the Perchloric Nitric Acid Method. 15 plants per treatment were analyzed to determine shoot iron content using an Inductively Coupled Plasma Optical Emission Spectrometer (Varian Medical Systems, Palo Alto, CA, USA).

Cloning and Constructs

Genomic DNA for cloning the *GmYSL7* promoter was extracted from mature soybean leaves using DNeasy Plant minikit (Qiagen). RNA was extracted from plant tissues using an RNeasy Plant mini kit (Qiagen) and cDNA synthesized using an iScript cDNA synthesis kit (Invitrogen). All constructs were PCR amplified from soybean nodule cDNA or gDNA using either Platinum Pfx50 (Invitrogen) or Phusion (Thermo Fisher Scientific) high fidelity polymerases and cloned using the Gateway cloning system (Invitrogen). A list of primers used can be found in Supplementary Table 3.

For GmYSL7 promoter GUS fusion constructs, a 2 kb genomic fragment immediately upstream of the GmYSL7 coding region was recombined into either pKGW-GGRR (Gavrin et al. 2016) or pKGWFS7 (Karimi et al., 2002). The full-length coding sequence of GmYSL7 was recombined into pGmLBC3-pK7GWIWG2 Gateway vector (Gavrin et al. 2016) to create a hairpin RNAi vector for silencing the gene. N-terminal GFP fusion constructs for GmYSL7 were constructed from the full-length coding sequence recombined into either pGmLBC3-pK7WGF2-R (Gavrin et al. 2016)

or a modified pK7WGF2 (pGmLBC3-pK7WGF2) where the 35S promoter is replaced by the GmLBC3 promoter. The free GFP construct was made by *Eco*RV digestion and re-ligation of the pGmLBC3-pK7WGF2 vector to remove the intervening Gateway cassette. For the symbiosome space GFP construct, MtNOD25 (Hohnjec et al. 2009) was PCR amplified from *M. truncatula* cDNA and recombined with pGmLBC3-pK7WGF2. For yeast expression, full length open reading frames of GmYSL7, AtYSL7, AtIRT1, AtOPT4 and ZmYS1 inserted into the pDR196GW vector.

The GmYSL7 coding sequence was synthesised with the MtYSL7 promoter and flanked by attL recombination sites inserted in the pUC57 (Synbio). The construct was recombined into pGBW13 using Gateway Cloning technology.

Transformation of Soybean and Medicago

Hairy root transformation of soybeans (cv Stevens) used *Agrobacterium rhizogenes* K599 and was as described by Mohammadi-Dehcheshmeh et al. (2014). Transformed roots were inoculated with *B. diazoefficiens* CB1809 (Becker Underwood, Somersby, NSW, Australia). Plants were grown under controlled temperature and lighting conditions (26°C day, 24°C night; 16 hr day; 120-150 µmol m^{-2} s^{-1}). Transformed nodules were examined 2-4 weeks post inoculation.

Transformation of *Medicago truncatula* was as described by Boisson-Dernier et al. (2001) using *A. rhizogenes* ARqua1.

Microscopy

Confocal imaging of GFP-fusion proteins was done on transgenic nodules either hand sectioned or sectioned in low melt agarose using a vibratome (752M Vibroslice, Campden Instruments, Loughborough, Leics., UK). In some instances, nodules were counterstained by FM4-64 (30 µg/ml). Nodule sections were immediately imaged as described previously (Limpens et al., 2009) using either an LSM Pascal 410 (Zeiss) or an SP5 II (Leica) confocal laser-scanning microscope.

Imaging of GUS expression was done as described in Clarke et al. (2015). Sections were either counterstained with ruthenium red or mounted directly in Milli-Q water,

and imaged using an Axiophot epifluorescence microscope with a set of Achroplan objective lens (Zeiss).

The protocol for tissue preparation for light and EM has been described previously (Limpens et al., 2009). Semithin sections (0.6 µm) for light microscopy and thin sections (60 nm) for EM of transgenic nodules were cut using a Leica Ultracut ultramicrotome UC7 (Leica). Sections were collected on 400 mesh nickel grids and examined using a Jeol JEM 1400 transmission electron microscope (Jeol Ltd, Tokyo, Japan).

Quantitative Reverse Transcription-PCR

RT-qPCR assays were used to measure transcript abundance in soybean tissues of control and YSL7 RNAi plants grown in sand or hydroponics. cDNA was synthesized from 500 ng total RNA using Iscript reverse transcriptase (Bio-Rad, Hercules, CA, USA), according to manufacturer's instructions. Quantitative real time PCR assays were done in a volume of 5 µl in triplicate and contained 1 µl of cDNA diluted 1/5, 1 X LightCycler® 480 SYBR green I mix (Roche Applied Science, Castle Hill, Australia) and 0.5 µM of each primer (GmYSL7 and GmUBI3 QRT primers; Supplementary Table 3). Assays were done using a LightCycler® 480 (Roche Applied Science) and the following conditions: 95°C 10 min, 45 cycles of 95°C 10 s, 56°C 10 s, 72°C 20 s, followed by ramping the temperature from 55°C to 95°C for melt curve analysis. PCR efficiency for each primer pair was determined using the LinRegPCR software (Ramakers et al., 2003) and data analysed using the LightCycler® 480 software package (Roche Applied Science). Data were normalized using *GmUBI3* (Glyma20g27950; Trevaskis *et al*., 2002) or *cons6* expression (Libault et al., 2008). Stable *GmUBI3* expression in the tissues examined in this study was confirmed through comparison of its expression with five characterized soybean reference genes (*cons4*, *6*, *7*, and *15*; Libault et al., 2008) using geNorm software (Vandesompele et al., 2002). The amplified product from the real-time reaction was cloned and sequenced to confirm the specificity of the amplification product.

Yeast complementation

To test for transport of Fe(II)NA AtYSL7, GmYSL7, ZmYS1 in pDR196GW and the empty vector were introduced into the yeast *fet3/fet4/ftr1* mutant (Spizzo et al. 1997;

DEY1530: *MATa ade2 his3 leu2 lys2 trp1 ura3 fet3-2::HIS3 fet4-1::LEU2 ftr1D1::TRP1*) using the method described by Dohmen et al. (1991). Fe(II)-NA plates were prepared by mixing 15 µl 10 mM $FeSO_4$ in 200 mM MES/Tris pH 7.4 with 250 µl 200 mM Na-ascorbate and 8 µl of 50 mM NA and heating at 65^{o}C for 10 minutes to produce a clear solution that was added to 25 ml of SD media to produce the Fe(II)-NA plate. Transformants were grown in liquid media to an OD600 of 1 and then serially spotted in ten-fold dilutions on either SD plates with no added iron, Fe(II)-NA plates or SD-plates with 10 µM Fe-citrate.

For the peptide transport assay AtOPT4, AtYSL7, GmYSL7 in pDR196GW and the empty vector were introduced into the yeast *opt1* mutant (Y11213: BY4742; *MATα; ura3Δ0; leu2Δ0; his3Δ1; lys2Δ0; YJL212c::kanMX4*, Euroscarf). Transformants were grown as above on minimal medium (0.17% YNB without amino acids and $(NH_4)_2SO_4$, supplemented with amino acids as required, and containing either 10 mM NH_4Cl (positive control) or 100 µM of the following peptides, ALAL, LSKL, IIGLM, KLLLLG, DRVYIHPF, DRVYIHPFHL or RLAPEGPDPHHN, as the sole source of nitrogen.

Syringolin A transport assay

An assay for transport of Syringolin A by AtYSL7 and GmYSL7 in the yeast strain Δ*pdr5* (Y12409: BY4742; *MATα; ura3Δ0; leu2Δ0; his3Δ1; lys2Δ0; YOR153w::kanMX4*, Euroscarf) was done as described in Hofstetter et al. (2013). Syringolin A was kindly provided by Robert Dudler, University of Zurich.

Statistical Analyses

A one-way ANOVA with Tukey's HSD (SAS Enterprise Guide Version 4.3; SAS Institute Inc., Cary, NC, USA) was used to analyze differences in plant organ dry mass after growth in varying Fe concentrations. Differences are reported as significant where $p < 0.05$.

RNAseq analysis of transcriptome in GmYSL7-RNAi nodules

The transcriptome for *GmYSL7*-RNAi nodules was compared to those transformed with an empty vector control using RNAseq. Hairy root transformation with pGmLBC3-pK7GWIWG2 vector or the vector containing *GmYSL7* coding sequence

was used to produce transformed nodules. RNA was isolated from nodules 21 or 22 days after inoculation using an RNeasy kit (Qiagen). Five replicates for each construct were done, each with nodules from 5-7 transformed plants. RNA integrity number (RIN) was determined on a 2100 bioanalyzer (Agilent) and was between 7 and 8.3 for all samples. RNAseq library construction and analysis were completed at Institute for Molecular Bioscience Sequencing Facility, The University of Queensland. A combination of the Ribo Zero rRNA removal bacteria (Illumina) and Ribo Zero rRNA removal plant (seed and root) (Illumina) was used to eliminate the rRNA from the sample. The library was constructed using a TruSeq® Stranded mRNA LT - SetA and SetB (Illumina). Sequencing was performed using the Illumina NextSeq500 (NextSeq control software v1.4/ Real Time Analysis v2.1). The library pool was diluted and denatured according to the standard NextSeq protocol, and sequenced to generate single-end 76 bp reads using a 75 cycle NextSeq500/550 High Output reagent Kit (Illumina).

Raw sequence reads were aligned to the JGI Wm82.a2 soybean assembly. DESeq2 (Love et al. 2014) was used to test for differential expression between control and YSL7-RNAi samples. Genes with $\log_2$ fold change ($\log_2$ FC) >1 and adjusted p-value < 0.05 were considered differentially expressed. Overrepresented biological terms were identified from the list of differentially expressed genes. GO term enrichment analysis was based on the information in SoyBase (https://soybase.org/). Enriched biological terms and their linkage were analysed and visualized using ClueGO v2.5.5 (Bindea et al., 2009), implemented in the Cytoscape v3.5.1 environment (Shannon et al., 2003; https://cytoscape.org/cy3.html). ClueGO parameters were as follow: Analysis Mode, Functional Analysis; Load Markers List, Glycine max (3847); Visual Style: Significance Shape, ellipse; ClueGO settings, Ontology/Pathway; GO, Biological Process / KEGG: downloaded the 12/12/2017; Evidence type, All Evidences; Statistical Test Used = Enrichment/Depletion (Two-sided hypergeometric test); Correction Method Used = Bonferroni step down; Min GO Level = 3, Max GO Level = 8, Min Percentage = 4.0, GO Fusion = true, GO Group = true, Kappa Score Threshold = 0.4; Over View Term = SmallestPValue; Group By Kappa Statistics = true; Initial Group Size = 1;Sharing Group Percentage = 50.0.

718 **Symbiosome isolation, SM and microsomal membrane isolation and proteomic**
719 **analysis.**

720 Symbiosomes were isolated as described by Clarke et al. (2015). SM was collected
721 after pelleting of the membrane and resuspended in 1M Urea for proteomic analysis.
722 Microsomal membrane was isolated from nodules ground and filtered through
723 miracloth as described in Clarke et al. (2015). Symbiosomes and other intact
724 organelles were pelleted by centrifugation at 20000 g. The membrane in the
725 supernatant (enriched in PM and endoplasmic reticulum) was collected by
726 centrifugation at 100,000 g for 1 hour at 4°C and the pellet resuspended in 8M Urea.
727 Proteomic analysis was completed at the La Trobe Comprehensive Proteomics
728 Platform (La Trobe University). Data were collected on a Q Exactive HF (Thermo-
729 Fisher Scientific) in Data Dependent Acquisition mode using *m*/*z* 350–1500 as MS
730 scan range at 60 000 resolution. HCD MS/MS spectra were collected for the 7 most
731 intense ions per MS scan at 60 000 resolution with a normalized collision energy of
732 28% and an isolation window of 1.4 *m*/*z*. Dynamic exclusion parameters were set as
733 follows: exclude isotope on, duration 30 s and peptide match preferred. Other
734 instrument parameters for the Orbitrap were MS maximum injection time 30 ms with
735 AGC target 3×10^6, MSMS for a maximum injection time of 110 ms with AGT target
736 of 1×10^5.
737

738 Raw files consisting of high-resolution MS/MS spectra were processed with
739 MaxQuant version 1.5.5.1 to detect features and identify proteins using the search
740 engine Andromeda. Sequence data for soybean from Phytozome
741 (https://phytozome.jgi.doe.gov/pz/portal.html#!info?alias=Org_Gmax) was used as
742 the database for the search engine**.**

743

744 **ACCESSION NUMBERS**

745 The accession number for *GmYSL7* is NM_001289202.2

746

747 **ACKNOWLEGMENTS**

We thank Catherine Curie for providing the plasmid containing ZmYS1 and useful discussions about YSL transporters and Sarah Conte and Elsbeth Walker for providing advice about the methods for yeast assays for transport of Fe(II)-NA.

SUPPLEMENTAL MATERIAL

Supplementary table S1. Unique GmYSL7 and GmNOD26 peptides[1] identified in purified symbiosome membrane, a microsomal membrane fraction, and a symbiosome-enriched membrane sample from soybean nodule homogenate.

Supplementary table S2. Genes upregulated or downregulated in GmYSL7-RNAi nodules and data for all genes expressed in the nodules.

Supplementary table S3. Primers used in this study.

Supplementary figure S1. Phylogenetic analysis of YSL proteins

Supplementary figure S2. Expression analysis of the YSL genes in soybean.

Supplementary figure S3. Expression of *GmYSL7* in response to Fe status during nodule development.

Supplementary figure S4. Detailed morphological analysis of determinate nodule development

Supplementary figure S5. FM 4-64 stained symbiosomes extracted from empty vector control and GmYSL7-RNAi nodules.

FIGURE LEGENDS

Figure 1. GmYSL7 is expressed in infected cells of soybean root nodules. A. Transcript level of *GmYSL7* in tissue samples from different organs. N, nodules; L, leaves; DNR, denodulated roots; R, roots. B. Transcript level of GmYSL7 during nodule development. 6R, roots 6 days after inoculation (DAI); 10RN, roots and nodules 10 DAI; 13N-26N, nodules the indicated DAI. Data shown are for three independent time courses. Bars, SE (n = 3). Nitrogenase activity was first detected at 18 DAI. C. Transgenic root expressing pYSL7:GFP-GUS. GUS staining was not detectable in the very early stages of nodule development. Arrowhead indicates a nodule initiation. D. Transgenic pYSL7:GFP-GUS 10-day-old nodule primordia. IR,

778 infected region. E. Transgenic pYSL7:GFP-GUS mature nodule. GUS staining is
779 restricted to infected cells. OC, outer cortex. F. Magnification of E. Scale bars, 150
780 µm.
781
782 **Figure 2. Localization of GmYSL7 in soybean nodule cells infected with rhizobia.**
783 A. GFP-GmYSL7 localizes on symbiosome membranes in infected cell of soybean
784 nodules. B. Colocalization of GFP-YSL7 with membrane lipophilic dye FM4-64 in
785 the same cell. IC, infected cell; NI, non-infected cell; ROI, region of interest. C.
786 Fluorescent intensity plot of ROI from B. D. Superimposed confocal image of GFP-
787 GmYSL7 signal on the symbiosome membrane in rhizobia-infected nodule cells. E.
788 Free GFP localizes to the cytoplasmic spaces surrounding symbiosomes in infected
789 cells. F. MtNOD25-GFP (Hohnjec et al. 2009) localizes to the peribacteroid space
790 inside the symbisomes. Scale bars, 5µm.
791
792 **Figure 3. RNAi silencing of GmYSL7 affects nodule development.** A. Transcript
793 level of GmYSL7 and its closest homologs in 24-day-old nodules of empty vector
794 control and RNAi-GmYSL7 plants (error bars represent SD; n=4; t-test: *, $p<0.05$).
795 B. Nitrogenase enzyme activity in 24-day-old nodules of empty vector control and
796 RNAi-GmYSL7 plants (error bars represent SD; n=8; t-test: **, $p<0.01$). C. Fresh
797 weight of 24-day-old nodules of empty vector control and RNAi-GmYSL7 (error bars
798 represent SD; t-test: *, $p<0.05$). D. Longitudinal section of a 24-day-old nodule from
799 an empty vector control plant. E. Magnification of (A) showing developed (stage IV)
800 infected cells. F. Electron microscopy of infected cells of a 24-day-old nodule from
801 empty vector control containing developed multibacteroid symbiosomes. G.
802 Longitudinal section of a RNAi-GmYSL7 24-day-old nodule. H. Magnification of (D)
803 showing undeveloped (stage II) infected cells. I. Electron microscopy of infected cells
804 of a RNAi-GmYSL7 24-day-old nodule containing undeveloped single-bacteroid
805 symbiosomes. Scale bars as indicated.
806
807 **Figure 4. RNAseq analysis of *GmYSL7*-RNAi nodules.** A. Principal component
808 analysis of RNAseq samples. B. Heatmap of clustering of differentially regulated
809 genes in each nodule sample. Gene-expression values are normalized by using a z-
810 score transformation on TPM. C, D. Gene Ontology enrichment analysis of biological
811 processes in up (C) and down (D) regulated genes from GmYSL7 RNAi nodules. GO

812 term enrichment analyses were performed using the ClueGO v2.5.5 plugin (Bindea et
813 al., 2009) in Cytoscape v3.5.1 (Shannon et al., 2003). Circles represent an enriched
814 group of genes based on their GO terms. Circle size and colour indicate the number of
815 mapped genes and associated Term PValue corrected with Bonferroni step down.
816
817 **Figure 5. GmYSL7 does not transport iron or Fe(II)-nicotianamine (NA).**
818 DEY1530 yeast (*fet3/fet4/ftr1*) was transformed with the empty vector plasmid
819 pDR196, *AtYSL7, GmYSL7* or *ZmYS1* in pDR196GW. Serial dilutions of each yeast
820 transformant were applied to SD plates (that include 1.6 μM $FeCl_3$) with 10 μM Fe-
821 citrate, Fe(II)-NA or no added iron (no iron) and the plates grown for 3-5 days.
822
823 **Figure 6. GmYSL7 and AtYSL7 transport oligopeptides.** *AtOPT4, AtYSL7,*
824 *GmYSL7* in pDR196GW and the empty vector (pDR196) were introduced into the
825 yeast *opt1* mutant, Y11213. Serial dilutions of each transformant were grown as
826 above on minimal medium containing either 10 mM NH_4Cl (positive control) or 100
827 μM peptide (with sequence as indicated) as the sole source of nitrogen
828
829 **Figure 7. GmYSL7 transports Syringolin** A. BY4742 yeast *Δpdr5:KanMX6*
830 transformed with the empty vector (pDR196) or the vector expressing *AtYSL7* or
831 *GmYSL7* were plated as a lawn on solid synthetic defined (SD) media. Filter disks
832 with the indicated SylA solutions were placed onto the plates and inhibition of growth
833 examined after 2 days.
834
835 **Figure 8. GmYSL7 is functionally equivalent to MtYSL7.** A. Growth of
836 representative wild type (WT), *ysl7-1*, and *ysl7-1* transformed with *GmYSL7*
837 controlled by the *MtYSL7* promoter (*ysl7-1 $MtYSL7_{prom}$:: GmYSL7*). Bar = 1 cm. B.
838 Dry weight of 28 dpi WT, *ysl7-1*, and *ysl7-1 $MtYSL7_{prom}$:: GmYSL7* plants. Data are
839 the mean ± SE of 5 transformed plants. C. Nitrogenase activity of 28 dpi WT, *ysl7-1*,
840 and *ysl7-1 $MtYSL7_{prom}$:: GmYSL7* plants. Acetylene reduction was measured in
841 duplicate from two sets of three-four pooled plants. Data are the mean ± SE. *
842 indicates statistically significant differences ($p<0.05$)
843
844
845

Parsed Citations

Abbamondi GR, De Rosa S, Iodice C, Tommonaro G (2014) Cyclic Dipeptides Produced by Marine Sponge-Associated Bacteria as Quorum Sensing Signals. Nat. Prod. Commun 9: 229-232
Pubmed: Author and Title
Google Scholar: Author Only Title Only Author and Title

Acuña G, Alvarez-Morales A, Hahn M, Hennecke H (1987) A vector for the site-directed, genomic integration of foreign DNA into soybean root-nodule bacteria. Plant Mol. Biol. 9: 41-50
Pubmed: Author and Title
Google Scholar: Author Only Title Only Author and Title

Avenhaus U, Cabeza RA, Liese R, Lingner A, Dittert K, Salinas-Riester G, Pommerenke C and Schulze J (2016) Short-Term Molecular Acclimation Processes of Legume Nodules to Increased External Oxygen Concentration. Front. Plant Sci. 6: 1133. doi: 10.3389/fpls.2015.01133
Pubmed: Author and Title
Google Scholar: Author Only Title Only Author and Title

Becana M, Wienkoop S, Matamoros MA (2018) Sulfur Transport and Metabolism in Legume Root Nodules. Front. Plant Sci. 9 :1434. doi:10.3389/fpls.2018.01434
Pubmed: Author and Title
Google Scholar: Author Only Title Only Author and Title

Bindea G, Mlecnik B, Hackl H, Charoentong P, Tosolini M, Kirilovsky A, Fridman WH, Pagès F, Trajanoski Z, Galon J (2009) ClueGO: a Cytoscape plug-in to decipher functionally grouped gene ontology and pathway annotation networks. Bioinformatics. 25: 1091-1093. doi: 10.1093/bioinformatics/btp101.
Pubmed: Author and Title
Google Scholar: Author Only Title Only Author and Title

Boisson-Dernier A, Chabaud M, Garcia F, Becard G, Rosenberg C, Barker DG (2001) Agrobacterium rhizogenes-transformed roots of Medicago truncatula for the study of nitrogen-fixing and endomycorrhizal symbiotic associations. Mol. Plant-Microbe Interact. 14: 695-700
Pubmed: Author and Title
Google Scholar: Author Only Title Only Author and Title

Brear EM, Day DA, Smith PMC (2013) Iron: an essential micronutrient for the legume–rhizobium symbiosis. Front. Plant Sci. 4: 359
Pubmed: Author and Title
Google Scholar: Author Only Title Only Author and Title

Broughton WJ, Dilworth MJ (1971) Control of leghemoglobin synthesis in snake beans. Biochem. J. 125: 1075-1080
Pubmed: Author and Title
Google Scholar: Author Only Title Only Author and Title

Cabeza R, Koester B, Liese R, Lingner A, Baumgarten V, Dirks J, Salinas-Riester G, Pommerenke C, Dittert K, Schulze J (2014) An RNA sequencing transcriptome analysis reveals novel insights into molecular aspects of the nitrate impact on the nodule activity of Medicago truncatula. Plant Physiol. 164: 400-11. doi: 10.1104/pp.113.228312.
Pubmed: Author and Title
Google Scholar: Author Only Title Only Author and Title

Catalano CM, Lane WS, Sherrier DJ (2004) Biochemical characterization of symbiosome membrane proteins from Medicago truncatula root nodules. Electrophoresis 25: 519-531
Pubmed: Author and Title
Google Scholar: Author Only Title Only Author and Title

Chu HH, Chiecko J, Punshon T, Lanzirotti A, Lahner B, Salt DE, Walker EL (2010) Successful Reproduction Requires the Function of Arabidopsis YELLOW STRIPE-LIKE1 and YELLOW STRIPE-LIKE3 Metal-Nicotianamine Transporters in Both Vegetative and Reproductive Structures. Plant Physiol. 154: 197-210
Pubmed: Author and Title
Google Scholar: Author Only Title Only Author and Title

Clarke VC, Loughlin PC, Day DA, Smith PMC (2014) Transport processes of the legume symbiosome membrane. Front. in Plant Sci. 5: 699. doi:10.3389/fpls.2014.00699
Pubmed: Author and Title
Google Scholar: Author Only Title Only Author and Title

Clarke VC, Loughlin PC, Gavrin A, Chen C, Brear EM, Day DA, Smith PMC (2015) Proteomic analysis of the soybean symbiosome identifies new symbiotic proteins. Mol. Cell Proteomics 14: 1301-1322
Pubmed: Author and Title
Google Scholar: Author Only Title Only Author and Title

Conte SS, Chu HH, Chan-Rodriguez D, Punshon T, Vasques KA, Salt DE, Walker EL (2013) Arabidopsis thaliana Yellow Stripe1-Like4 and Yellow Stripe1-Like6 localize to internal cellular membranes and are involved in metal ion homeostasis. Front. Plant Sci. 4: 283. doi:10.3389/fpls.2013.00283

Pubmed: Author and Title
Google Scholar: Author Only Title Only Author and Title

Curie C, Panaviene Z, Loulergue C, Dellaporta SL, Briat JF, Walker EL (2001) Maize yellow stripe1 encodes a membrane protein directly involved in Fe(III) uptake. Nature. 409: 346-349. doi: 10.1038/35053080.
Pubmed: Author and Title
Google Scholar: Author Only Title Only Author and Title

Curie C, Cassin G, Couch D, Divol F, Higuchi K, Jean M, Misson J, Schikora A, Czernic P, Mari S (2009) Metal movement within the plant: contribution of nicotianamine and yellow stripe 1-like transporters. Ann. Bot. 103: 1-11
Pubmed: Author and Title
Google Scholar: Author Only Title Only Author and Title

Dai J, Wang NQ, Xiong HC, Qiu W, Nakanishi H, Kobayashi T, Nishizawa NK, Zuo YM (2018) The Yellow Stripe-Like (YSL) Gene Functions in Internal Copper Transport in Peanut. Genes 9: 635. doi:10.3390/genes9120635
Pubmed: Author and Title
Google Scholar: Author Only Title Only Author and Title

Divol F, Couch D, Conéjéro G, Roschzttardtz H, Mari S, Curie C (2013) The Arabidopsis YELLOW STRIPE LIKE4 and 6 Transporters Control Iron Release from the Chloroplast. Plant Cell 25: 1040-1055
Pubmed: Author and Title
Google Scholar: Author Only Title Only Author and Title

Dohmen RJ, Strasser AWM, Honer CB, Hollenberg CP (1991) An efficient transformation procedure enabling long-term storage of competent cells of various yeast genera. Yeast 7: 691-692
Pubmed: Author and Title
Google Scholar: Author Only Title Only Author and Title

Fowler D, Coyle M, Skiba U, Sutton MA, Cape JN, Reis S, Sheppard LJ, Jenkins A, Grizzetti B, Galloway JN, Vitousek P, Leach A, Bouwman AF, Butterbach-Bahl K, Dentener F, Stevenson D, Amann M, Voss M (2013) The global nitrogen cycle in the twenty-first century. Philos. Trans. R. Soc. B-Biol. Sci. 368
Pubmed: Author and Title
Google Scholar: Author Only Title Only Author and Title

Gavrin A, Chiasson D, Ovchinnikova E, Kaiser BN, Bisseling T, Fedorova EE (2016) VAMP721a and VAMP721d are important for pectin dynamics and release of bacteria in soybean nodules. New Phytol. 210:1011-21
Pubmed: Author and Title
Google Scholar: Author Only Title Only Author and Title

Gavrin A, Kaiser BN, Geiger D, Tyerman SD, Wen Z, Bisseling T, Fedorova EE (2014) Adjustment of Host Cells for Accommodation of Symbiotic Bacteria: Vacuole Defunctionalization, HOPS Suppression, and TIP1g Retargeting in Medicago. Plant Cell 26: 3809-3822
Pubmed: Author and Title
Google Scholar: Author Only Title Only Author and Title

González-Guerrero M, V. E, Sáez Á, Tejada-Jiménez M (2016) Transition metal transport in plants and associated endosymbionts. Arbuscular mycorrhizal fungi and rhizobia. Front. Plant Sci. 7: 1088
Pubmed: Author and Title
Google Scholar: Author Only Title Only Author and Title

Hastwell AH, Gresshoff PM, Ferguson BJ. (2015) Genome-wide annotation and characterization of CLAVATA/ESR (CLE) peptide hormones of soybean (Glycine max) and common bean (Phaseolus vulgaris), and their orthologues of Arabidopsis thaliana. J Exp Bot. 66: 5271-87. doi: 10.1093/jxb/erv351.
Pubmed: Author and Title
Google Scholar: Author Only Title Only Author and Title

Hofstetter SS, Dudnik A, Widmer H, Dudler R (2013) Arabidopsis YELLOW STRIPE-LIKE7 (YSL7) and YSL8 Transporters Mediate Uptake of Pseudomonas Virulence Factor Syringolin A into Plant Cells. Mol. Plant-Microbe Interact. 26: 1302-1311
Pubmed: Author and Title
Google Scholar: Author Only Title Only Author and Title

Hohnjec N, Lenz F, Fehlberg V, Vieweg MF, Baier MC, Hause B, Küster H (2008) The Signal Peptide of the Medicago truncatula Modular Nodulin MtNOD25 Operates as an Address Label for the Specific Targeting of Proteins to Nitrogen-Fixing Symbiosomes. Mol. Plant-Microbe Interact. 22: 63-72
Pubmed: Author and Title
Google Scholar: Author Only Title Only Author and Title

Karimi M, Inze D, Depicker A (2002) GATEWAY((TM)) vectors for Agrobacterium-mediated plant transformation. Trends Plant Sci. 7: 193-195
Pubmed: Author and Title
Google Scholar: Author Only Title Only Author and Title

Kiers ET, Rousseau RA, West SA, Denison RF (2003) Host sanctions and the legume-rhizobium mutualism. Nature 425: 78-81
Pubmed: Author and Title
Google Scholar: Author Only Title Only Author and Title

Krusell L, Krause K, Ott T, Desbrosses G, Kramer U, Sato S, Nakamura Y, Tabata S, James EK, Sandal N, Stougaard J, Kawaguchi M, Miyamoto A, Suganuma N, Udvardi MK (2005) The sulfate transporter SST1 is crucial for symbiotic nitrogen fixation in Lotus japonicus root nodules. Plant Cell 17: 1625-1636

Pubmed: Author and Title
Google Scholar: Author Only Title Only Author and Title

Libault M, Thibivilliers S, Bilgin DD, Radwan O, Benitez M, Clough SJ, Stacey G (2008) Identification of Four Soybean Reference Genes for Gene Expression Normalization. Plant Genome 1: 44-54

Pubmed: Author and Title
Google Scholar: Author Only Title Only Author and Title

Limpens E, Ivanov S, van Esse W, Voets G, Fedorova E, Bisseling T (2009) Medicago N2-Fixing Symbiosomes Acquire the Endocytic Identity Marker Rab7 but Delay the Acquisition of Vacuolar Identity. Plant Cell 21: 2811-2828

Pubmed: Author and Title
Google Scholar: Author Only Title Only Author and Title

Liu T, Zeng JQ, Xia KF, Fan T, Li YG, Wang YQ, Xu XL, Zhang MY (2012) Evolutionary expansion and functional diversification of oligopeptide transporter gene family in rice. Rice 5: 12. doi:10.1186/1939-8433-5-12

Pubmed: Author and Title
Google Scholar: Author Only Title Only Author and Title

Love MI, Huber W, Anders S (2014) Moderated estimation of fold change and dispersion for RNA-seq data with DESeq2. Genome Biol 15:550.

Pubmed: Author and Title
Google Scholar: Author Only Title Only Author and Title

Lubkowitz M (2011) The Oligopeptide Transporters: A Small Gene Family with a Diverse Group of Substrates and Functions? Mol Plant 4: 407-415

Pubmed: Author and Title
Google Scholar: Author Only Title Only Author and Title

Mohammadi-Dehcheshmeh M, Ebrahimie E, Tyerman SD, Kaiser BN (2014) A novel method based on combination of semi-in vitro and in vivo conditions in Agrobacterium rhizogenes-mediated hairy root transformation of Glycine species. In Vitro Cell. Dev. 50: 282-291.

Pubmed: Author and Title
Google Scholar: Author Only Title Only Author and Title

Mohd-Noor SN, Day DA and Smith PMC (2015) Chapter 68: The Symbiosome Membrane. In: Biological Nitrogen Fixation. Volume 2. Ed. Frans de Bruijn. P683-694 Wiley-Blackwell. ISBN: 978-1-118-63704-3.

Pubmed: Author and Title
Google Scholar: Author Only Title Only Author and Title

Pessi G, Ahrens CH, Rehrauer H, Lindemann A, Hauser F, Fischer HM, Hennecke H (2007) Genome-wide transcript analysis of Bradyrhizobium japonicum bacteroids in soybean root nodules. Mol. Plant-Microbe Interact. 20: 1353-1363

Pubmed: Author and Title
Google Scholar: Author Only Title Only Author and Title

Ramakers C, Ruijter JM, Deprez RHL, Moorman AFM (2003) Assumption-free analysis of quantitative real-time polymerase chain reaction (PCR) data. Neurosci. Lett. 339: 62-66

Pubmed: Author and Title
Google Scholar: Author Only Title Only Author and Title

Reid DE, Ferguson BJ, Gresshoff PM (2011) Inoculation- and nitrate-induced CLE peptides of soybean control NARK-dependent nodule formation. Mol Plant Microbe Interact. 24:606-18. doi: 10.1094/MPMI-09-10-0207.

Pubmed: Author and Title
Google Scholar: Author Only Title Only Author and Title

Saier MH (2000) Families of transmembrane transporters selective for amino acids and their derivatives. Microbiology 146: 1775-1795

Pubmed: Author and Title
Google Scholar: Author Only Title Only Author and Title

Sasaki A, Yamaji N, Xia JX, Ma JF (2011) OsYSL6 Is Involved in the Detoxification of Excess Manganese in Rice. Plant Physiol. 157: 1832-1840

Pubmed: Author and Title
Google Scholar: Author Only Title Only Author and Title

Schaaf G, Ludewig U, Erenoglu BE, Mori S, Kitahara T, von Wiren N (2004) ZmYS1 functions as a proton-coupled symporter for phytosiderophore- and nicotianamine-chelated metals. J. Biol. Chem. 279: 9091-9096

Pubmed: Author and Title
Google Scholar: Author Only Title Only Author and Title

Schmutz J, Cannon SB, Schlueter J, Ma J, Mitros T, Nelson W, Hyten DL, Song Q, Thelen JJ, Cheng J, Xu D, Hellsten U, May GD, Yu Y, Sakurai T, Umezawa T, Bhattacharyya MK, Sandhu D, Valliyodan B, Lindquist E, Peto M, Grant D, Shu S, Goodstein D, Barry K, Futrell-Griggs M, Abernathy B, Du J, Tian Z, Zhu L, Gill N, Joshi T, Libault M, Sethuraman A, Zhang X-C, Shinozaki K, Nguyen HT, Wing RA, Cregan P, Specht J, Grimwood J, Rokhsar D, Stacey G, Shoemaker RC, Jackson SA (2010) Genome sequence of the palaeopolyploid

soybean. Nature 463: 178-183
Pubmed: Author and Title
Google Scholar: Author Only Title Only Author and Title

Schneider S, Schintlmeister A, Becana M, Wagner M, Woebken D, Wienkoop S (2019) Sulfate is transported at significant rates through the symbiosome membrane and is crucial for nitrogenase biosynthesis. Plant Cell Environ. 42: 1180–1189. doi:10.1111/pce.13481
Pubmed: Author and Title
Google Scholar: Author Only Title Only Author and Title

Severin AJ, Woody JL, Bolon YT, Joseph B, Diers BW, Farmer AD, Muehlbauer GJ, Nelson RT, Grant D, Specht JE, Graham MA, Cannon SB, May GD, Vance CP, Shoemaker RC (2010) RNA-Seq Atlas of Glycine max: A guide to the soybean transcriptome. BMC Plant Biol. 10 10: 160. doi:10.1186/1471-2229-10-160
Pubmed: Author and Title
Google Scholar: Author Only Title Only Author and Title

Shannon P, Markiel A, Ozier O, Baliga NS, Wang JT, Ramage D, Amin N, Schwikowski B, Ideker T (2003) Cytoscape: A Software Environment for Integrated Models of Biomolecular Interaction Networks. Genome Res 13: 2498–2504
Pubmed: Author and Title
Google Scholar: Author Only Title Only Author and Title

Smith PM, Atkins CA (2002) Purine biosynthesis. Big in cell division, even bigger in nitrogen assimilation. Plant Physiol.;128: 793–802. doi:10.1104/pp.010912
Pubmed: Author and Title
Google Scholar: Author Only Title Only Author and Title

Spizzo T, Byersdorfer C, Duesterhoeft S, Eide D. (1997) The yeast FET5 gene encodes a FET3-related multicopper oxidase implicated in iron transport. Mol Gen Genet. 256: 547–556. doi:10.1007/pl00008615
Pubmed: Author and Title
Google Scholar: Author Only Title Only Author and Title

Stacey MG, Patel A, McClain WE, Mathieu M, Remley M, Rogers EE, Gassmann W, Blevins DG, Stacey G (2008) The Arabidopsis AtOPT3 protein functions in metal homeostasis and movement of iron to developing seeds. Plant Physiol. 146: 589-601
Pubmed: Author and Title
Google Scholar: Author Only Title Only Author and Title

Thompson JD, Higgins DG, Gibson TJ (1994) CLUSTAL W: improving the sensitivity of progressive multiple sequence alignment through sequence weighting, position-specific gap penalties and weight matrix choice. Nucleic Acids Res. 22: 4673–4680. doi:10.1093/nar/22.22.4673
Pubmed: Author and Title
Google Scholar: Author Only Title Only Author and Title

Trevaskis B, Wandrey M, Colebatch G, Udvardi MK (2002) The soybean GmN6L gene encodes a late nodulin expressed in the infected zone of nitrogen-fixing nodules. Mol. Plant-Microbe Interact. 15: 630-636
Pubmed: Author and Title
Google Scholar: Author Only Title Only Author and Title

Udvardi M, Poole PS (2013) Transport and Metabolism in Legume-Rhizobia Symbioses. Annu. Rev. Plant Biol. 64: 781-805
Pubmed: Author and Title
Google Scholar: Author Only Title Only Author and Title

Udvardi MK, Day DA (1997) Metabolite transport across symbiotic membranes of legume nodules. Annu. Rev. Plant Physiol. Plant Mol. Biol. 48: 493-523
Pubmed: Author and Title
Google Scholar: Author Only Title Only Author and Title

Unkovich M, Baldock J (2008) Measurement of a symbiotic N2 fixation in Australian agriculture. Soil Biol. Biochem. 40: 2915-2921
Pubmed: Author and Title
Google Scholar: Author Only Title Only Author and Title

Vance CP (2001) Symbiotic nitrogen fixation and phosphorus acquisition. Plant nutrition in a world of declining renewable resources. Plant Physiol., 127: 390–397.
Pubmed: Author and Title
Google Scholar: Author Only Title Only Author and Title

Van de Velde W, Zehirov G, Szatmari A, Debreczeny M, Ishihara H, Kevei Z, Farkas A, Mikulass K, Nagy A, Tiricz H, Satiat-Jeunemaitre B, Alunni B, Bourge M, Kucho K-i, Abe M, Kereszt A, Maroti G, Uchiumi T, Kondorosi E, Mergaert P (2010) Plant Peptides Govern Terminal Differentiation of Bacteria in Symbiosis. Science 327: 1122-1126
Pubmed: Author and Title
Google Scholar: Author Only Title Only Author and Title

Vandesompele J, De Preter K, Pattyn F, Poppe B, Van Roy N, De Paepe A, Speleman F (2002) Accurate normalization of real-time quantitative RT-PCR data by geometric averaging of multiple internal control genes. Genome Biol. 3
Pubmed: Author and Title
Google Scholar: Author Only Title Only Author and Title

Vida TA, Emr SD (1995) A new vital stain for visualizing vacuolar membrane dynamics and endocytosis in yeast. J. Cell Biol. 128: 779-792

Pubmed: Author and Title
Google Scholar: Author Only Title Only Author and Title

Wienkoop S, Saalbach G (2003) Proteome analysis. Novel proteins identified at the peribacteroid membrane from Lotus japonicus root nodules. Plant Physiol. 131: 1080-1090

Pubmed: Author and Title
Google Scholar: Author Only Title Only Author and Title

Xu C, Nadon BD, Kim KD, Jackson SA (2018) Genetic and epigenetic divergence of duplicate genes in two legume species. Plant, Cell Environ. 41: 2033-2044

Pubmed: Author and Title
Google Scholar: Author Only Title Only Author and Title

Yen MR, Tseng YH, Saier MH (2001) Maize Yellow Stripe1, an iron-phytosiderophore uptake transporter, is a member of the oligopeptide transporter (OPT) family. Microbiology 147: 2881-2883

Pubmed: Author and Title
Google Scholar: Author Only Title Only Author and Title